Alzheimer's Research & Therapy

RESEARCH

Open Access

CHIT1 and DDAH1 levels relate to amyloid-related imaging abnormalities risk profile in Alzheimer's disease patients

Marlies Oosthoek[1*], Everard G.B. Vijverberg[2], Elena R. Blujdea[1], Sjors G.J.G. In't Veld[1,3], Martín Pucheu Avilés[1,3], Sára E. Zsadanyi[4,5], Yanaika S. Hok-A-Hin[1], Allerdien Visser[3], Wiesje M. van der Flier[2], Frederik Barkhof[6,7], Marta del Campo[8], Martijn C. Schut[3], Alexandre Bejanin[4,5], Daniel Alcolea[4,5], Charlotte E. Teunissen[1] and Lisa Vermunt[1]

Abstract

Background Amyloid-related imaging abnormalities (ARIA) are a common and potentially dangerous side effect in anti-amyloid therapies, creating a need for tools to assess ARIA risk. Several patient factors have been linked to ARIA; namely the presence of microbleeds (MBL^+), *APOE E4* carriership ($APOE4^+$), and extremely low CSF Aβ42 concentrations (A^L). We hypothesize that studying the CSF proteome of Alzheimer's disease (AD) dementia patients from a high-risk group ($MBL^+APOE4^+A^L$) can inform on the biological underpinnings of ARIA risk and aid the progress of ARIA risk biomarkers.

Methods We utilized CSF proteomic data of AD ($n=156$) and cognitively unimpaired individuals (CU $n=100$) of the Amsterdam Dementia Cohort. The proteome of the defined high-risk ($n=13$) was compared to low-risk AD group ($n=23$), using age and sex corrected linear regressions followed by gene ontology analysis. For biomarker prioritization, we selected proteins that were abnormal in the high-risk group versus low-risk and CU patients. The biomarkers were validated in an independent cohort (high risk $n=14$, low risk $n=9$) analyzed using customized multiplex panels. Lastly, we assessed biomarker lead co-expression.

Results Ninety-four proteins differentiated in the high-risk group compared to low-risk ($p<0.05$), none surviving FDR correction. These proteins were enriched for synapse-related proteins and axonogenesis. CHIT1 (vs. low-risk AD: FC = 1.0, $p=0.014$, vs. CU: FC = 2.4, $p<0.001$) and DDAH1 (vs. low-risk AD: FC=-0.31, $p=0.046$, vs. CU: FC = 0.5, $p<0.001$) were prioritized as biomarker. DDAH1 protein changes replicated in an independent cohort (FC=-0.37, $p=0.010$), and CHIT1 replicated on a trend level (FC = 0.70, $p=0.104$). DDAH1 levels had the highest co-expression with synaptic process, energy utilization and RNA-binding cell signaling related proteins ($R>0.8$).

Conclusions The findings suggest that in the high risk group, there is a lack of upregulation in synapse and axonogenesis related proteins. High CSF CHIT1 and less increased CSF DDAH1 levels within AD relate to ARIA risk. From the literature, the link to ARIA risk for CHIT1 could be its contribution to innate immunity or vascular amyloid

*Correspondence:
Marlies Oosthoek
m.c.oosthoek@amsterdamumc.nl

Full list of author information is available at the end of the article

deposition, and for DDAH1 to blood-brain barrier integrity. Biomarker assays are available to assess the potential of CHIT1 and DDAH1 in trials and treatment studies in the clinical setting.

Keywords ARIA, Biomarker, Risk

Background

Monoclonal antibodies targeting amyloid β (Aβ), one of the main hallmarks of Alzheimer's disease (AD), are becoming available as an AD therapy [1–4]. The major side effect of these therapies is amyloid-related imaging abnormalities (ARIA) [5]. ARIA is detected with magnetic resonance imaging (MRI) and presents as either microhemorrhages or superficial siderosis (ARIA-H) or vasogenic edema or sulcal effusions (ARIA-E) [5, 6]. ARIA events have been reported in 10–40% of patients in various clinical trials targeting amyloid or related processes with antibodies and are independent of clinical drug efficacy [1, 3, 4, 7–9]. The severity of these ARIA events can vary greatly, ranging from little or no symptoms (around 70% of the cases), to (in a few cases) death [10–12]. This highlights the unmet need for tools that assist clinicians in accurately predicting the risk of developing mild and severe forms of ARIA.

Although the exact etiology of ARIA remains unclear, it is hypothesized to be related to the induced innate inflammatory response by the therapy to vascular amyloid deposition [13]. This leads to leakage of the blood vessels/capillaries which can be captured on the MRI as ARIA-E or ARIA-H. As the first anti-amyloid therapies were only recently approved there is still a sparsity of real-world post-treatment data on studying ARIA risk [14]. Clinical trials data has linked several risk factors to the development of ARIA, in particular the presence of microbleeds (MBL^+), *APOE E4* carriership ($APOE4^+$), very high amyloid PET load, and extremely low CSF Aβ42 (A^L) [15–18]. Using these risk factors as a proxy, we hypothesize that we need to define an extreme risk phenotype, where multiple risk factors are present as an indicator of common etiology, to capture the proteome changes relevant to ARIA risk and aid in an initial understanding of the biological underpinnings of ARIA risk [19, 20].

CSF proteomics are an effective method to study disease biology and identify novel biomarkers for neurological diseases. CSF has less interference from other body systems compared to blood and due to the close proximity to the brain it can also be more sensitive to changes in the central nervous system. Additionally, CSF testing has been implemented in specialized clinical care for AD [21]. Recent advancements in multiplex affinity-based proteomics have driven large-scale biomarker discovery and have expedited translation to antibody-based laboratory tests that can be implemented in clinical settings [22–25]. In the current study, we leverage a large discovery study to characterize the CSF proteome of the AD dementia extreme phenotype ($MBL^+APOE4^+A^L$) group. We compare these patients to their extreme phenotype counterpart– the lowest risk group in AD ($MBL^-APOE4^-A^U$) - and to cognitively unimpaired elderly with a normal CSF AD biomarker profile, no microbleeds and not carrying the *APOE E4* allele. The rationale for including a comparison against controls in the biomarker discovery stage is that a good biomarker for ARIA should reflect a biological state that is not or only weakly present in controls. This prioritized novel biomarker leads that were validated in an independent cohort on customized biomarker panels. Altogether, the aim is to provide novel insight into the CSF biology related to ARIA risk and define a CSF biomarker for ARIA risk, that will subsequently facilitate future ARIA risk studies.

Methods

Participants

For the discovery cohort, all AD dementia ($n = 156$) and cognitively unimpaired individuals (CU, $n = 100$) with available data on microbleeds, *APOE E4* genotype, CSF Aβ42 levels, and CSF PEA proteomics from the Amsterdam Dementia Cohort (ADC) were included [26, 27]. The validation cohort consisted of the selection of mild cognitive impairment due to AD (MCI $n = 17$) and AD dementia patients ($n = 6$) from the ADC ($n = 16$) and the Sant Pau Initiative on Neurodegeneration (SPIN) cohort ($n = 7$) with available biomarker data and defined as extreme high or low risk profile (described in next paragraph) [28]. All participants underwent cognitive and neurological assessments and magnetic resonance imaging (MRI). Diagnoses were made during the multidisciplinary meeting according to consensus criteria [29, 30]. Ethical approval was given at the local review boards. Written informed consent was provided by all study participants or a representative.

CSF measurements of Aβ42, total Tau (tTau) and phosphorylated Tau (pTau) 181 were performed locally using commercially available kits and drift corrected (ADC: Innotest, Fujirebio, SPIN: Lumipulse G600 automated platform) [31]. A positive AD biomarker profile was defined locally (ADC: Aβ42 < 813 pg/mL, pTau181 > 51 pg/mL, and tTau > 375 pg/mL, tTau/Aβ ratio > 0.46, positivity was based on the ratio; SPIN: Aβ42/Aβ40 ratio < 0.062, tTau > 456 pg/mL and pTau > 63 pg/mL positivity was based on all biomarkers) [32, 33]. The symptomatic AD group had an abnormal CSF AD biomarker profile and the CU group had a normal CSF AD

biomarker profile (ADC: ratio negative; SPIN negative on all markers).

Risk factors were scored in two manners (Fig. 1). Firstly, for initial analysis to determine correlated proteins based on the individual risk factor in AD patients, microbleeds were scored based on the number of MBLs, where the total number was available ($n = 150$). Zero MBLs, resulted in 0 points; 1 MBL in 1 point, 2 or 3 MBLs in 2 points; and 4 or more MBLs in 3 points [34, 35]. APOE4 genotype was categorized based on the number of APOE4 alleles (0, 1 or 2) and Aβ42 measurements were used as a continuous measure.

Within AD patients, an extreme risk profile was defined. This was based on dichotomized risk factors. Microbleeds were stratified by the presence of at least one microbleed (discovery cohort $MBL^{+} n = 33$; $MBL^{-} n = 123$) as one microbleed already resulted in an increased risk in patients receiving Donanamab [36]. *APOE E4* status was split by carriership of at least one *E4* allele (discovery cohort $APOE4^{+} n = 96$; $APOE4^{-} n = 60$). Aβ42 levels were separated based on the median within the AD group, in a cohort dependent manner (Discovery cohort $A^{LOWER\ (L)} n = 79$; $A^{UPPER\ (U)}$, $n = 77$; *Discovery cohort: 605 pg/mL; Validation ADC cohort: 610 pg/mL; Validation SPIN cohort: 522 pg/mL*). This allowed for definition of the extreme high and low risk profiles of the discovery cohort ($MBL^{+}APOE4^{+}A^{L} n = 13$; $MBL^{-}APOE4^{-}A^{U} n = 23$) and the validation cohort ($MBL^{+}APOE4^{+}A^{L} n = 14$; $MBL^{-}APOE4^{-}A^{U} n = 9$). This resulted in 23 patients in the low risk group and 13 patients in the high risk group. We conducted sensitivity analysis in the discovery cohort including only patients with 4 or less microbleeds ($n = 7$ in the high risk group) to test generalizability according to the appropriate use criteria [37]. Additionally, we included an analysis to determine translatability based on the MMSE score by focusing only on patients with an MMSE score between 20 and 28[7]. This resulted in 16 patients in the discovery cohort (high $n = 3$, low $n = 13$). In the validation cohort there were a total of 19 patients (high $n = 13$, low $n = 6$) with an MMSE score between

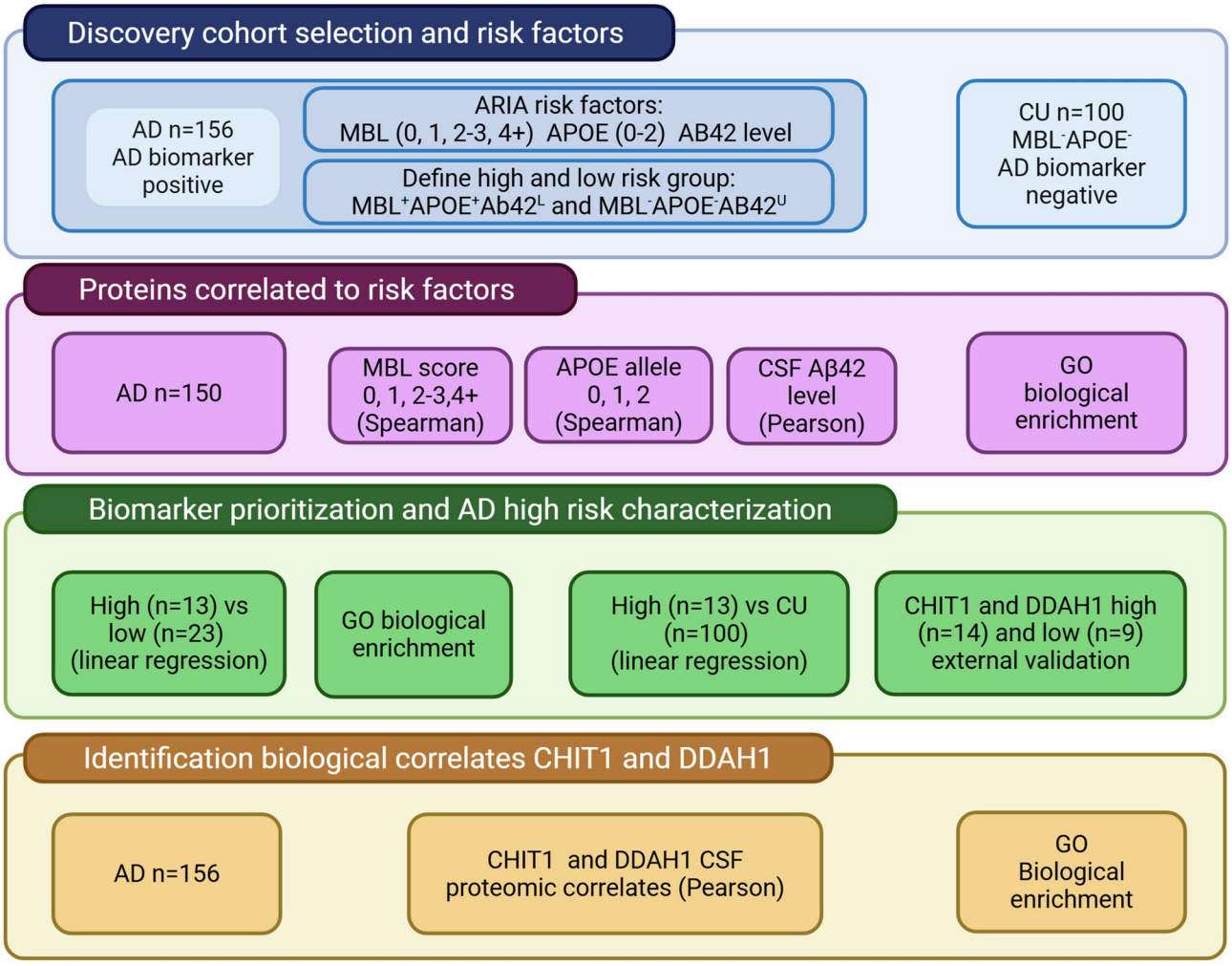

Fig. 1 Study overview. Created in https://BioRender.com

20 and 28. One splicing variant outlier of CHIT1 was deleted, resulting in 12 patients with a high risk group.

MRI assessments

An MRI was performed using a 1.0T, 1.5T, or 3T whole-body MRI scanner (Siemens Magnetom Impact, GE Healthcare; Signa, HDXT; Ingenuity TF PET/MR, Philips Medical Systems; Titan, Toshiba Medical Systems) according to previously described standardized protocols [26]. MBLs were defined as small, homogenous hypointensities smaller than 10 mm [38]. They were counted throughout the brain on the transverse T2* susceptibility-sensitive sequence by an experienced neuroradiologist or trained personnel. Fazekas scores were determined using fluid-attenuated inversion recovery (FLAIR) according to previously described scoring: 1 is punctate foci, 2 is beginning confluence, and 3 is large confluent areas [26, 39].

CSF proteomics

CSF was obtained by lumbar puncture, collected in polypropylene tubes and biobanked according to published guidelines [40]. In short, samples were centrifuged *2000 x g* for 10 min at room temperature. CSF was aliquoted in polypropylene tubes and stored at -80 °C until further analysis.

Proteins in the discovery cohort were measured using antibody-based proximity extension assay (PEA) technology. This included the measurement of 979 proteins with all available 96 Target multiplex panels, described in detail in our previous study [22]. In short, the PEA method employs oligonucleotide-bound antibodies. When both antibodies bind the target protein, the oligonucleotides are in proximity forming the basis for a quantitative real-time polymerase chain reaction (qPCR). Protein expression levels were determined in normalized protein expression (NPX) values, which is an inverse $\log_2$ scale, meaning that when the difference is 1, the levels are twice as high. Only assays with at least 85% of the samples above the lower limit of detection were included in the analysis [22]which resulted in 642 unique proteins.

CSF external validation on custom multiplex panels

The validation cohort was measured with custom multiplex panels optimized for CSF as described in our previous studies [22, 23, 41]. In short, each plate contained four CSF quality control samples, a negative control, calibrators used for normalization, and samples. The lower limit of detection per plate was determined at three times the noise from the negative control. These panels have been validated in independent patient cohorts for discrimination of AD from CU individuals [22, 23]. Protein expression levels in these panels were presented as NPX values.

Statistical and biological enrichment analysis

All statistical analyses were performed in R version 4.3.2. Demographic group differences were determined using a t-test or chi-square test where appropriate.

In the discovery cohort, there were 12 values ($n = 4$ CU, $n = 8$ AD) of CHIT1 that were close to 0 NPX. These values were imputed using the mice package in R [42]. The values were imputed using predictive mean matching. None of the imputations were in the defined extreme risk profile groups.

Protein correlates of individual risk factors were identified using Spearman correlation with the MBL score (score 0, 1, 2 or 3) and APOE alleles (score 0, 1 or 2) and Pearson for the CSF Aβ42 levels (Figure 1). Analyses were performed using the scored risk factor classification indicated above, including only AD patients in the analyses. FDR multiple testing correction was applied. Proteins were further characterized with gene ontology (GO) analysis using the ClusterProfiler package [43]. The background was set to the 642 unique proteins included in the original correlation analysis. Due to this analysis step's explorative and hypothesis-generating nature, we used proteins with the standard p-value cut-off of 0.05 as input for the biological enrichment. Significant GO terms had a q-value < 0.05.

For the biological characterization of $MBL^{+}APOE4^{+}A^{L}$ patients, this group was compared to the low risk - $MBL^{-}APOE4^{-}A^{U}$ - group using age and sex corrected linear regression analysis (Figure 1). The output was used to perform GO analysis with a similar approach as described above. All proteins with $p < 0.05$ were included in the GO-analysis and the background was set to the 642 unique proteins included in the analysis. A follow-up analysis was performed based on the differential proteins from the high vs. low analysis for the ARIA risk biomarker identification and selection. The $MBL^{+}APOE4^{+}A^{L}$ patients were compared to CU individuals using age and sex corrected linear regression. FDR multiple testing correction was applied and set at q-value < 0.05. Biomarker findings were validated using an independent validation cohort with proteins measured on custom multiplex protein panels, following similar statistical analysis. To strengthen the assessment of the results, we used the beta coefficients and the standard error of the beta coefficients from the linear regression models to perform a meta-analysis using the two cohorts. We performed a random-effects analysis using the metafor R package.

We used Pearson correlation analysis to test the association of our lead biomarkers with the proteomics data to further explore the biological correlates. Correlation analyses were only performed in the AD dementia patients. Correlation coefficients of (R) > 0.5/-0.5 were considered moderate and $R > 0.7$/-0.7 were considered strong [44]. FDR multiple testing correction was

applied. Post hoc GO analysis was performed on the top 10 correlated proteins for CHIT1 and proteins with an $R > 0.8$/-0.8 for DDAH1. All 642 proteins included in the correlation analyses were included as the background and significantly enriched terms had a q-value < 0.05. We performed an extra analysis using z-scored median NPX per sample as a covariate in the linear regression model. Median NPX value can be used to investigate the general protein load.

Results

Clinical characteristics

AD patients were significantly older and had lower MMSE scores compared to the CU group (Table 1). Additionally, the Fazekas scores were significantly higher in the AD population compared to the CU group. Specifically focusing on the defined high ($MBL^+APOE4^+A^L$) or low ($MBL^-APOE4^-A^U$) ARIA risk AD patients in the discovery cohort, there were no significant differences in age and MMSE scores. The Fazekas score was higher in the high risk group. There were no clinical difference between the high and low risk groups of the validation cohort.

Correlation analyses per risk factor

MBL score was weakly correlated ($p < 0.05$) with the levels of 18 proteins (Supplemental Table 1) in AD patients. APOE4 genotype was weakly correlated ($p < 0.05$) with 14 proteins. Aβ42 measurements weakly correlated ($p < 0.05$) with 33 proteins. However, there were no enriched GO terms for any of these correlations. None of the correlation analyses survived FDR-correction.

Biological analysis of defined highest versus lowest risk group within AD patients

Biological differences of the risk factors were investigated based on the differential protein abundance of the $MBL^+APOE4^+A^L$ versus $MBL^-APOE4^-A^U$ AD patients. Ninety-four proteins were nominally significant ($p < 0.05$), yet none survived FDR-correction. Two were increased and the other 92 were decreased in the high risk group (Fig. 2A; Supplemental Table 2). In the sensitivity analysis with a maximum of 4 microbleeds, 78 of the 94 proteins remained significant. In the GO enrichment analysis, the 94 nominally significant proteins were further investigated. No molecular functions were enriched. Synapse, glutamatergic synapse, and asymmetric synapse were enriched cellular components (Fig. 2B, q < 0.05). All enriched biological processes also related to the synapse and axonogenesis; regulation of neuron projection development, positive regulation of axonogenesis, synapse assembly, regulation of axonogenesis, positive regulation of cell projection organization (Fig. 2C, q < 0.05).

Discovery of CSF CHIT1 and DDAH1 levels as potential biomarkers for ARIA risk

Ideally, the ARIA risk biomarker would also differentiate from CU individuals. To realize this, we focused only on the 94 proteins that were identified in the

Table 1 Patient demographics

	Discovery cohort				Validation cohort	
	Control	AD dementia	AD dementia		AD dementia	
			Highest risk	Lowest risk	Highest risk	Lowest risk
n	100	156	13	23	14	9
Age	57 (8)****	66 (8)****	70 (7)	68 (8)	70 (4)	68 (6)
Sex, F (%)	34 (34%)	59 (38%)	5 (38%)	6 (26%)	4 (29%)	2 (22%)
MMSE	28 (2)****	20 (5)****	17 (4)	19 (6)	24 (3)	23 (5)
Diagnosis						
MCI due to AD	0 (0%)	0 (0%)	0 (0%)	0 (0%)	10 (71%)	7 (78%)
AD dementia	0 (0%)	156 (100%)	13 (100%)	23 (100%)	4 (29%)	2 (22%)
Microbleeds	0 (0%)	33 (21%)	13 (100%)	0 (0%)	14 (100%)	0 (0%)
Fazekas scores	0.45 (0.6)****	1.03 (0.9)****	1.92 (1.0)*	1.00 (0.9)*		
APOE4						
E2/E2	1 (1%)	0 (0%)	0 (0%)	0 (0%)	0 (0%)	0 (0%)
E2/E3	16 (16%)	3 (2%)	0 (0%)	1 (4%)	0 (0%)	1 (11%)
E2/E4	0 (0%)	1 (0.6%)	1 (8%)	0 (0%)	0 (0%)	0 (0%)
E3/E3	83 (83%)	57 (37%)	0 (0%)	22 (96%)	0 (0%)	8 (89%)
E3/E4	0 (0%)	61 (40%)	3 (23%)	0 (0%)	9 (64%)	0 (0%)
E4/E4	0 (0%)	34 (22%)	9 (69%)	0 (0%)	5 ((36%)	0

Numerical variables are shown as mean (SD). P-values were calculated with t-tests and chi-square tests. Percentages are given as a percentage within a diagnosis group. Highest risk is defined as patients with microbleeds, APOE4 carriers and Aβ42 levels below the median. Lowest risk is defined is defined as patients without microbleeds, no APOE4 carriers and Aβ42 levels above the median. F = female; MMSE = mini-mental state examination; MCI = mild cognitive impairment; AD = Alzheimer's disease

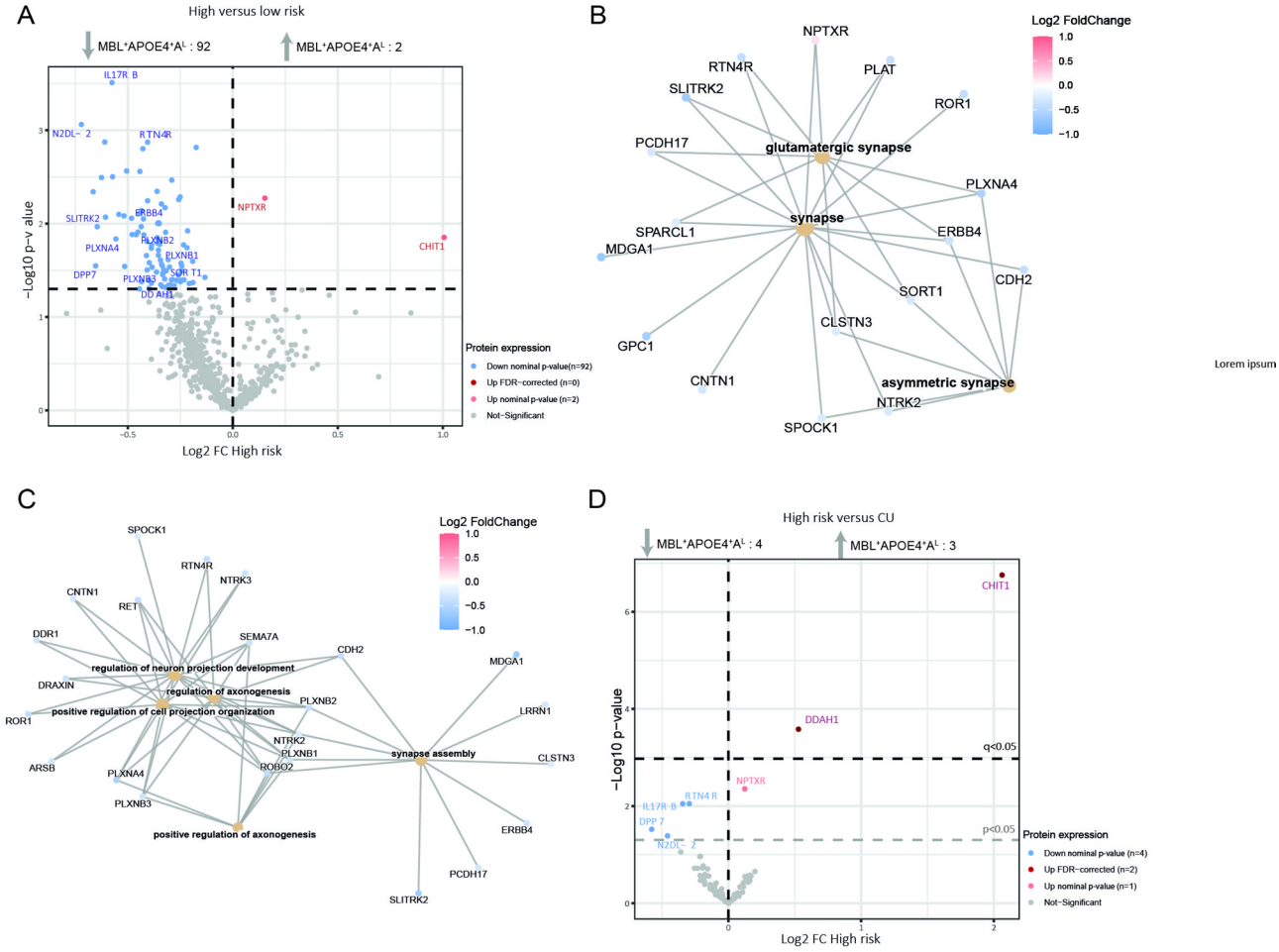

Fig. 2 CSF characterization of extreme risk group. (**A**) Volcano plot with differentially expressed proteins in CSF for MBL^{+}APOE4^{+}A^{Lower} (high risk) versus MBL^{-}APOE4^{-}A^{Upper} (low risk) AD dementia patients. The x-axis show the beta coefficients (log2 foldchange) and the y-axis shows the p-value. All proteins with a $p < 0.05$ are indicated in blue (downregulated) and red (upregulated), the horizontal line indicated the $p < 0.05$ threshold. P values were calculated using a linear regression analysis with age and sex correction. Network plot of significantly enriched (**B**) cellular components and (**C**) biological processes. Colored dots of the proteins indicate the log2 foldchange, where red indicates it is increased in the high risk group and blue indicates it is decreased in the high risk group compared to the low risk group based on the nominal p-value. GO-terms were significant when q < 0.05. (**D**) Volcano plot with differentially expressed proteins in CSF for MBL^{+}APOE4^{+}A^{Lower} (high risk) AD dementia patients versus CU individuals. The x-axis show the beta coefficients (log2 foldchange) and the y-axis shows the p-value. All proteins with a $p < 0.05$ are indicated in blue (downregulated) and red (upregulated), the horizontal line indicated the $p < 0.05$ threshold. FDR-corrected significant proteins are indicated in a darker shade. P values were calculated using a linear regression analysis with age and sex correction, followed by an FDR multiple testing correction

differential expression analysis of MBL^{+}APOE4^{+}A^{L} versus MBL^{-}APOE4^{-}A^{U}. The 94 proteins were compared between the MBL^{+}APOE4^{+}A^{L} and CU groups (Fig. 2D; Supplemental Table 2). Seven proteins were nominally different between MBL^{+}APOE4^{+}A^{L} and CU. CHIT1 and DDAH1 survived FDR-correction. CHIT1 is increased in the high risk group ($\beta = 1.006$, $p = 0.014$; Fig. 3A) and DDAH1 is decreased in the high risk group (β=-0.305, $p = 0.046$; Fig. 3B) compared to low risk AD patients and both were upregulated in high risk versu CU. To give an indication about the translatability to eligible patients with a maximum of 4 microbleeds, DDAH1 showed and effects size of -0.476 and CHIT1 showed an effect size of 1.00 in the high versus low comparison of this subgroup.

CHIT1 and DDAH1 clinical and biological correlates

Correlation analyses between the two most promising markers and all proteins included in the proteomic analysis were performed to provide context into the general processes they are associated with (Supplemental Table 3). CHIT1 levels showed significant correlations with 490 proteins (q < 0.05). However, all correlation coefficients were between − 0.3 and 0.4, indicating weak to modest correlation strength. The strongest correlations were with VASN ($R = 0.40$, q = 0.0001), SMOC2 ($R = 0.38$, q = 0.0002), LILRB2 ($R = 0.37$, q = 0.0002), LYVE1 ($R = 0.37$, q = 0.0002), and IL-18BP ($R = 0.37$, q = 0.0002). Post hoc GO analysis on the top 10 correlated proteins showed no enriched terms.

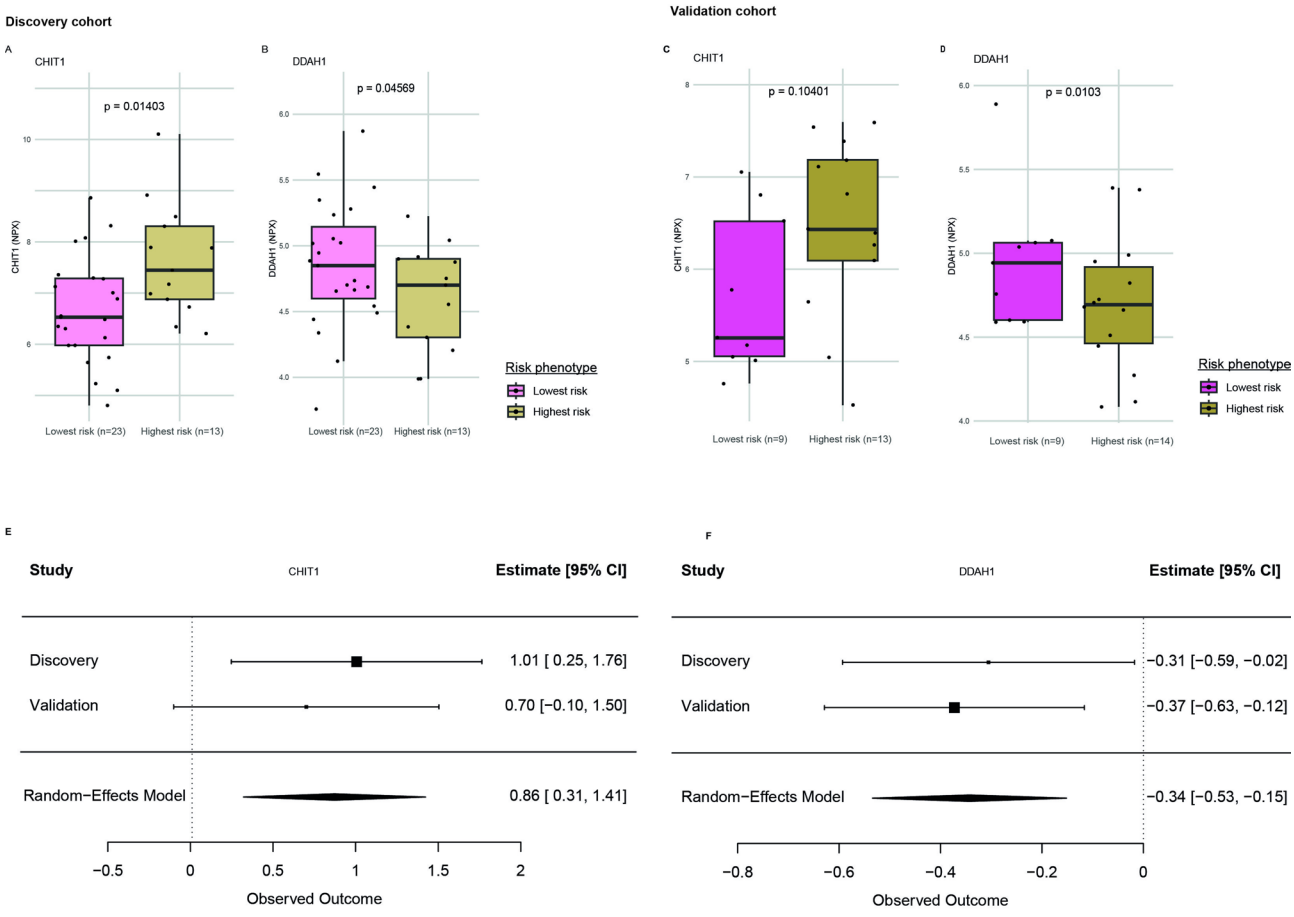

Fig. 3 Boxplots of potential CSF biomarkers for ARIA risk. Concentrations of the proteins that were differentially expressed in the MBL^{+}APOE4^{+}A^{Lower} (high risk) versus MBL^{-}APOE4^{-}A^{Upper} and CU individuals as determined with linear regression are shown for the discovery (**A**-**B**) and validation (**C**-**D**) cohort. In pink the low risk group and in beige the high risk group. Meta-analyzed cohort results for CHIT1 (**E**) and DDAH1 (**F**).

DDAH1 levels were correlated with 614 proteins (q < 0.05) of which 108 had a strong correlation ($R > 0.7$). The strongest correlations were with LRRN1 ($R = 0.88$, q < 0.0001), IGF1R ($R = 0.88$, q < 0.0001), GALNT2 ($R = 0.88$, q < 0.0001), CLSTN3 ($R = 0.87$, q < 0.0001), and SCAMP3 ($R = 0.87$, q < 0.0001). We performed post hoc GO-analysis on the proteins with an R below −0.8 or above 0.8 ($n = 30$) and found several processes to be enriched (Fig. 4). Enriched molecular functions related to energy utilization and cell signaling (Fig. 4A) and cellular components and biological processes relate to synaptic structure and development (Fig. 4B/C). An additional analysis with z-scored median NPX value per sample as a covariate in the linear regression model resulted in similar findings for both CHIT1 and DDAH1.

External validation of CHIT1 and DDAH1 on customized multiplex panels

We validated CHIT1 and DDAH1 as candidate ARIA risk markers in an independent cohort of AD patients using custom multiplex panels [22, 23]. In line, there was a trend of increased CHIT1 ($p = 0.104$) and significantly decreased DDAH1 ($p = 0.010$) in the highest risk group compared to the lowest risk group (Fig. 3C-D). We performed a meta-analysis showing the overall effects across the two cohorts. There is an overall increase in CHIT1 levels with an estimate of 0.86 95%CI [0.31–1.41] (Fig. 3E) and an overall decrease with an estimate of -0.34 95%CI [-0.53- -0.15] of DDAH1 (Fig. 3F). To be included in clinical trials, patients required an MMSE score between 20 and 28. We also performed a meta-analysis including patients within this range. The random effects model gives an estimate of 0.89 with a 95%CI [0.04–1.73] for CHIT1 and −0.38 with a 95%CI [-0.65 - -0.11] for DDAH1.

Discussion

In the current study, we investigated how predetermined risk factor profiles for ARIA affected the CSF proteome to gain insights into the CSF biology of ARIA risk. We discovered two new potential biomarkers (CHIT1 and DDAH1) that may hold promise for ARIA risk prediction

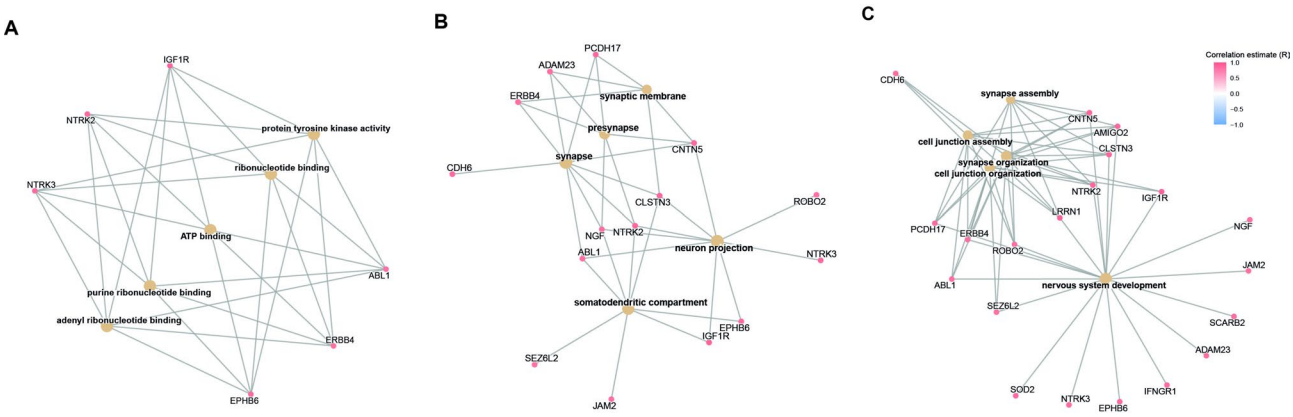

Fig. 4 Correlation analyses with DDAH1 and CHIT1. Networks of enriched GO-terms for (**A**) molecular function, (**B**) cellular components, and (**C**) biological processes. Pearson correlation analysis between DDAH1 and all proteins were performed. All proteins with a correlation coefficient $R > 0.8$ and FDR corrected $q < 0.05$ were included in the GO analysis. Colored dots with the proteins indicate the correlation coefficient, where red indicates a positive correlation and blue indicates a negative correlation

tools. High risk AD patients showed lower CSF protein levels related to the synapse and axonogenesis compared to low risk AD patients. CHIT1 levels positively correlated with microbleeds. DDAH1 covaried with proteins enriched for synapse and neuron development related processes, as well as energy utilization and RNA-binding cell signaling related proteins, which highlights that these markers may cover distinct biological aspects of ARIA risk. The available custom panels would allow broad testing of their value as more clinical samples will become available.

Here, we showed that patients with a high risk of developing ARIA may have lower levels of axonogenesis and synapse related protein levels, specifically protein levels related to the glutamatergic and asymmetric synapse were reduced or failed to upregulate. The glutamatergic synapse is known to be affected in AD and is one of the major excitatory neurons involved in learning and memory [45]. Astrocytes are important regulators in the homeostasis of glutamate, synaptic plasticity and memory in general [46, 47]. We postulate that a reduction in these proteins in CSF could be indicative of astrocytic impairment, especially considering that the majority of the proteins which drove the significant GO-terms (PLXNA4, ERBB4, NTRK4, PLXNB1, and PLXNB2) are mainly expressed by astrocytes [48, 49]. Research in mice has indicated that there is a compensatory response of astrocytes to the loss of smooth muscle cells following anti-amyloid therapy [50]. Although the exact nature (pro- or anti-inflammatory) of this response needs to be further investigated, a disrupted homeostatic state can make the brain predisposed to ARIA events. Plexins (e.g. PLXNA4, PLXNB1, PLXNB2) are important proteins in synaptic plasticity, epithelial repair, pro-inflammatory responses, and glial cell communication and were also shown to be downregulated in the high risk group [51, 52]. Combined these findings suggest that the downregulation of these proteins may play a role in the insufficient compensatory response to treatment, resulting in ARIA events.

DDAH1 is the most common of two isoforms of dimethylarginine dimethylaminohydrolase (DDAH), its main function is to metabolize asymmetric (N(G), N(G))-dimethylarginine (ADMA) [53]. This induces an increase in nitric oxide (NO) levels, a signaling molecule with multiple functions (ADMA-NO pathway) [54]. NO can cause vasodilation, stimulate an immune response, and is involved in neurotransmission, apoptosis, gene transcription, and post-translation protein modification [55]. DDAH1 is widely expressed throughout the body, and in the brain it is mainly expressed by neurons and endothelial cells [56]. The downstream effects of reduced DDAH1 levels may be reflected in the strongest co-expression proteins that were enriched for lower synaptic development, energy metabolism, and cell signaling, and possibly also enrichment for lower synaptic processes in the characterization of the high risk phenotype. A sensitivity analysis adjusting for median protein level (z-scored median NPX level) yielded similar biological results. Following stroke, increased DDAH1 levels have been shown to promote neurogenesis and induce ischemic tolerance, which is suggestive for neuroprotective functioning of DDAH1 [54, 57]. DDAH1 has also been shown to protect against blood-brain-barrier (BBB) leakage, and it has been shown that a disruption of the ADMA-NO pathway can induce brain edema [56, 58]. In line, a recent study on AD molecular subtypes, one subtype is characterized by BBB dysfunction and this is the subtype with low DDAH1 levels [59]. In relation to ARIA risk, it is conceivable that the low CSF DDAH1 levels may be suggestive of BBB dysfunction, and a reduced capacity to exhibit neuroprotective functions once the treatment is started.

CHIT1 levels are increased in several neurodegenerative diseases [60]. Within the brain it is mostly expressed in the white matter, but generally it is expressed by activated macrophages [48, 49, 61]. It plays an important role in the innate immunity and aids in the clearance of chitinous organisms [62, 63]. Furthermore, it has been shown to play a role in reactive gliosis, but a protective effect of CHIT1 in AD has also been reported, by regulating microglial activation and reducing neuronal apoptosis [63, 64]. Research on ARIA in mice showed an increase in the infiltration of perivascular macrophages and peripheral monocytes, which results in microhemorrhagic lesions [13]. We postulate that increased CHIT1 levels in CSF may be a sign of an activated innate immune response or perhaps pre-existent increased infiltration of macrophages and monocytes, which, following treatment, primes the perivascular macrophages to the response seen in ARIA.

This study is the first to investigate the effect of ARIA risk profile on the CSF proteome of AD patients. There are methodological considerations that should be noted. First, due to the sparsity of patient data of ARIA cases, we used a proxy for ARIA risk by comparing extreme phenotypes. However, we hypothesized that by defining an extreme risk profile, we are able to identify the underlying proteomic profile of the combined effects of the risk factors. This is similar to how autosomal dominant AD can be relevant as an extreme and well-defined phenotype for sporadic AD [65, 66]. Here we showed that by taking this approach we were able to identify differences in the proteome and prioritize two potential ARIA risk biomarkers. In addition, we cannot make the distinction between ARIA-H and ARIA-E, while it could be affected by different biological risk factors. Furthermore, while the initial cohort was large, with over 200 individuals, the extreme risk phenotype groups were small, including less than 20 patients per group. Therefore, the statistical power was limited and as such we could not systematically adjust for multiple testing. This limits our ability to detect other potential proteins of interest and warrants extra caution with the interpretation of these results due to the risk of false positive findings. Eligibility for receiving treatment is based on the number of microbleeds and MMSE score. Our analysis including only eligible patients based on first the maximum of 4 MBL followed by the MMSE score indicate our results are also translatable to the in trials included population. For the biomarker analyses, we used an independent validation cohort with an orthological assay, highlighting the validity of the prioritized markers. For CHIT1 it is important to acknowledge that a small subset of patients have alternative splice variants [67]due to which the protein is not detected by the antibodies (5%). Notably, the CHIT1 values in these splice variant carriers is so low that is cannot be confused with a low value that fits with the low risk phenotype. Moreover, none of these variants were in the discovery analysis comparing the extreme risk groups, indicating that these results were not influenced by the different variants.

Conclusion

In this study, we suggest CHIT1 and DDAH1 as potential biomarkers for an ARIA risk screening tool. We provide background on the potential roles of these markers in ARIA and indicate how they can relate to the increased risk. Besides clinical replication and the association with AD, CHIT1 and DDAH1 have good cross-technology robustness, (i.e., CSF Olink and untargeted Mass Spectrometry DDAH1 $R = 0.70$, CHIT1 $R = 0.69$; CSF Olink and Somascan DDAH1 $R = 0.91$, CHIT1 $R = 0.89$) [68]. Altogether, our findings justify investigating the performance of these assays and the applicability as an ARIA risk screening tool in a research context in treated patients and be critically assessed for added value compared to MRI, plasma and genetic tools. This step is technically very feasible, because custom PEA panels (CHIT1 and DDAH1), and singleplex immunoassays (ELISA: CHIT1) were designed for scalable application [69]. Accurately predicting individuals at risk of developing ARIA could greatly improve the impact of the medication and smoothen the patient selection and monitoring processes.

Abbreviations

AD	Alzheimer's disease
ADC	Amsterdam Dementia cohort
ADMA	Asymmetric (N(G), N(G))-dimethylarginine
APOE4	APOE E4 genotype
ARIA	Amyloid related imaging abnormalities
ARIA-E	ARIA- Edema
ARIA-H	ARIA– micro hemorrhagic lesions or superficial siderosis
Aβ	Amyloidβ
BBB	Blood brain barrier
CSF	Cerebrospinal fluid
CU	Cognitively unimpaired
DDAH	Dimethylarginine dimethylaminohydrolase
FC	Fold change
GO	Gene ontology
MBL	Microbleeds
$MBL^{+}APOE4^{+}A^{L}$	Highest risk group
$MBL^{-}APOE4^{-}A^{U}$	Lowest risk group
MCI	Mild cognitive impairment
MRI	Magnetic resonance imaging
NO	Nitric oxide
NPX	Normalized protein expression
pTau	Phosphorylated tau
qPCR	Quantitative real-time polymerase chain reaction
SPIN	Sant Pau Initiative on Neurodegeneration
tTau	Total Tau

Supplementary Information

The online version contains supplementary material available at https://doi.org/10.1186/s13195-025-01799-3.

Supplementary Material 1

Acknowledgements
Not applicable.

Author contributions
M.O., L.V., and C.E.T. designed the study. E.R.B., S.G.J.G.V, M.C.S, M.P.A., and A.V. contributed to the statistical analysis and figures. L.V., E.G.B.V., W.M.v.d.F., D.A., A.B. recruited participants and collected data and samples. Y.S.H. and M.d.C. prepared samples for proteomic analysis. E.G.B.V., S.E.Z., and F.B. contributed to the MRI data. M.O. and L.V. drafted the manuscript. E.G.B.V. and C.E.T. were major contributors to the writing of the manuscript. All authors read and contributed to the revisions and editing of this manuscript.

Funding
The PRIDE study was supported by Alzheimer Nederland (WE.03-2018-05, M.d.C. and C.E.T.) and Selfridges Group Foundation (NR170065, M.d.C. and C.E.T.). The SPIN cohort received funding from the Fondo de Investigaciones Sanitario (FIS), Instituto de Salud Carlos III (PI21/00791, PI14/01126, PI17/01019, PI20/01473, PI13/01532, PI16/01825, PI18/00335, PI19/00882, PI18/00435, PI22/00611, INT19/00016, INT23/00048, PI17/01896, AC19/00103, CP20/00038, and PI22/00307) and the CIBERNED program (Program 1, Alzheimer Disease to AL), jointly funded by Fondo Europeo de Desarrollo Regional, Unión Europea, "Una manera de hacer Europa". The SPIN cohort was also supported by the National Institutes of Health (NIA grants 1R01AG056850-01A1; R21AG056974; and R01AG061566), by Generalitat de Catalunya (2017-SGR-547, SLT006/17/125, SLT006/17/119, SLT002/16/408), "Marató TV3" foundation grants 20141210, 044412 and 20142610, a grant from the Fundació Bancaria La Caixa (DABNI project), Fundació Catalana Síndrome de Down and Fundació Víctor Grífols i Lucas, the Alzheimer's Association (AARG-22-923680) and the Ajuntament de Barcelona, in collaboration with Fundació La Caixa (23S06157-001).

Data availability
Data is available upon reasonable request by contacting the corresponding author.

Declarations

Consent for publication
Not applicable.

Competing interests
The authors declare no competing interests.

Ethical approval and consent to participate
Ethical approval was given at the local review boards (Amsterdam Dementia Cohort: AD CSF biobank METC number 00–211; SPIN cohort: COLLECTION 16/2013). Written informed consent was provided by all study participants or a representative.

Author details
[1]Neurochemistry Laboratory, Department of Laboratory Medicine, Amsterdam Neuroscience, Vrije Universiteit Amsterdam, Amsterdam UMC, De Boelelaan 1117, Amsterdam 1081 HV, The Netherlands
[2]Alzheimer Center, Department of Neurology, Vrije Universiteit Amsterdam, Amsterdam UMC, De Boelelaan 1117, Amsterdam 1081 HV, The Netherlands
[3]Translational AI in Laboratory Medicine, Department of Laboratory Medicine, Vrije Universiteit Amsterdam, Amsterdam UMC, De Boelelaan 1117, Amsterdam 1081 HV, The Netherlands
[4]Sant Pau Memory Unit, Department of Neurology, Institut d'Investigacions Biomèdiques Sant Pau Hospital de Sant Pau, Universitat Autònoma de Barcelona, Barcelona, Spain
[5]Center of Biomedical Investigation Network for Neurodegenerative Diseases (CIBERNED), C. de Melchor Fernández Almagro 3, Madrid 28029, Spain
[6]Department of Neuroinflammation, Queen Square MS Centre, UCL Queen Square Institute of Neurology, Faculty of Brain Science, University College of London, London WC1E 6BT, UK
[7]Department of Radiology and Nuclear Medicine, Vrije Universiteit Amsterdam, Amsterdam UMC, De Boelelaan 1117, Amsterdam 1081 HV, The Netherlands
[8]BarcelonaBeta Brain Research Center (BBRC), Pasqual Maragall Foundation, C/ de Wellington, 30, Barcelona 08005, Spain

Received: 11 April 2025 / Accepted: 25 June 2025
Published online: 22 July 2025

References

1. Mintun MA, et al. Donanemab in early Alzheimer's disease. N Engl J Med. 2021;384:1691–704. https://doi.org/10.1056/NEJMoa2100708.
2. Pontecorvo MJ, et al. Association of Donanemab treatment with exploratory plasma biomarkers in early symptomatic Alzheimer disease: A secondary analysis of the TRAILBLAZER-ALZ randomized clinical trial. JAMA Neurol. 2022. https://doi.org/10.1001/jamaneurol.2022.3392.
3. van Dyck CH, et al. Lecanemab in early Alzheimer's disease. N Engl J Med. 2022. https://doi.org/10.1056/NEJMoa2212948.
4. Budd Haeberlein S, et al. Two randomized phase 3 studies of aducanumab in early Alzheimer's disease. J Prev Alzheimer's Disease. 2022;9:197–210. https://doi.org/10.14283/jpad.2022.30.
5. Sperling RA, et al. Amyloid-related imaging abnormalities in amyloid-modifying therapeutic trials: recommendations from the Alzheimer's association research roundtable workgroup. Alzheimer's Dement. 2011;7:367–85. https://doi.org/10.1016/j.jalz.2011.05.2351.
6. Barakos J, et al. MR imaging features of Amyloid-Related imaging abnormalities. Am J Neuroradiol. 2013;34:1958. https://doi.org/10.3174/ajnr.A3500.
7. Sims JR, et al. Donanemab in early symptomatic Alzheimer disease: the TRAILBLAZER-ALZ 2 randomized clinical trial. JAMA. 2023;330:512–27. https://doi.org/10.1001/jama.2023.13239.
8. Swanson CJ, et al. A randomized, double-blind, phase 2b proof-of-concept clinical trial in early Alzheimer's disease with lecanemab, an anti-Aβ protofibril antibody. Alzheimers Res Ther. 2021;13:80. https://doi.org/10.1186/s13195-021-00813-8.
9. Salloway S, et al. A phase 2 multiple ascending dose trial of bapineuzumab in mild to moderate Alzheimer disease. Neurology. 2009;73:2061. https://doi.org/10.1212/WNL.0b013e3181c67808.
10. Reish NJ, et al. Multiple cerebral hemorrhages in a patient receiving Lecanemab and treated with t-PA for stroke. N Engl J Med. 2023;388:478–9.
11. Castellani RJ, et al. Neuropathology of Anti-Amyloid-β immunotherapy: A case report. J Alzheimers Dis. 2023;93:803–13. https://doi.org/10.3233/JAD-221305.
12. Solopova E, et al. Fatal iatrogenic cerebral β-amyloid-related arteritis in a woman treated with Lecanemab for Alzheimer's disease. Nat Commun. 2023;14:8220. https://doi.org/10.1038/s41467-023-43933-5.
13. Taylor X, et al. Amyloid-β (Aβ) immunotherapy induced microhemorrhages are associated with activated perivascular macrophages and peripheral monocyte recruitment in Alzheimer's disease mice. Mol Neurodegeneration. 2023;18:59. https://doi.org/10.1186/s13024-023-00649-w.
14. Alzforum L. Side Effects No Worse in Clinical Use Than They Were in Trial, <https://www.alzforum.org/news/conference-coverage/leqembi-side-effects-no-worse-clinical-use-they-were-trial (2024).
15. Joseph-Mathurin N, et al. Amyloid-Related imaging abnormalities in the DIAN-TU-001 trial of gantenerumab and solanezumab: lessons from a trial in dominantly inherited Alzheimer disease. Ann Neurol. 2022;92:729–44. https://doi.org/10.1002/ana.26511.
16. Barakos J, et al. Detection and management of Amyloid-Related imaging abnormalities in patients with Alzheimer's disease treated with Anti-Amyloid Beta therapy. J Prev Alzheimers Dis. 2022;9:211–20. https://doi.org/10.14283/jpad.2022.21.
17. Jeong SY et al. Incidence of Amyloid-Related Imaging Abnormalities in Patients With Alzheimer Disease Treated With Anti-β-Amyloid Immunotherapy: A Meta-analysis. Neurology. 2022;99:e2092-e2101. https://doi.org/10.1212/wnl.0000000000201019
18. Doran SJ, Sawyer RP. Risk factors in developing amyloid related imaging abnormalities (ARIA) and clinical implications. Front Neurosci. 2024;18:1326784. https://doi.org/10.3389/fnins.2024.1326784.
19. De Kort AM, et al. Decreased cerebrospinal fluid amyloid β 38, 40, 42, and 43 levels in sporadic and hereditary cerebral amyloid angiopathy. Ann Neurol. 2023;93:1173–86. https://doi.org/10.1002/ana.26610.
20. Hu H, et al. Deciphering the role of APOE in cerebral amyloid angiopathy: from genetic insights to therapeutic horizons. Ann Med. 2025;57:2445194. https://doi.org/10.1080/07853890.2024.2445194.

21. Teunissen CE, et al. White paper by the society for CSF analysis and clinical neurochemistry: overcoming barriers in biomarker development and clinical translation. Alzheimers Res Ther. 2018;10:30. https://doi.org/10.1186/s13195-018-0359-x.
22. del Campo M, et al. CSF proteome profiling across the Alzheimer's disease spectrum reflects the multifactorial nature of the disease and identifies specific biomarker panels. Nat Aging. 2022;2:1040–53. https://doi.org/10.1038/s43587-022-00300-1.
23. Hok-A-Hin YS et al. Large-scale CSF proteome profiling identifies biomarkers for accurate diagnosis of frontotemporal dementia. MedRxiv, 2024.2008.2019.24312100 (2024). https://doi.org/10.1101/2024.08.19.24312100
24. del Campo M, et al. CSF proteome profiling reveals biomarkers to discriminate dementia with lewy bodies from Alzheimer´s disease. Nat Commun. 2023;14:5635. https://doi.org/10.1038/s41467-023-41122-y.
25. Hok AHYS, et al. Thimet oligopeptidase as a potential CSF biomarker for Alzheimer's disease: A cross-platform validation study. Alzheimers Dement (Amst). 2023;15:e12456. https://doi.org/10.1002/dad2.12456.
26. van der Flier WM, et al. Optimizing patient care and research: the Amsterdam dementia cohort. J Alzheimers Dis. 2014;41:313–27. https://doi.org/10.3233/jad-132306.
27. van der Flier WM, Scheltens P. Amsterdam dementia cohort: performing research to optimize care. J Alzheimers Dis. 2018;62:1091–111. https://doi.org/10.3233/JAD-170850.
28. Alcolea D, et al. The Sant Pau initiative on neurodegeneration (SPIN) cohort: A data set for biomarker discovery and validation in neurodegenerative disorders. Alzheimers Dement (N Y). 2019;5:597–609. https://doi.org/10.1016/j.trci.2019.09.005.
29. Dubois B, et al. Research criteria for the diagnosis of Alzheimer's disease: revising the NINCDS-ADRDA criteria. Lancet Neurol. 2007;6:734–46. https://doi.org/10.1016/s1474-4422(07)70178-3.
30. McKhann GM, et al. The diagnosis of dementia due to Alzheimer's disease: recommendations from the National Institute on Aging-Alzheimer's association workgroups on diagnostic guidelines for Alzheimer's disease. Alzheimers Dement. 2011;7:263–9. https://doi.org/10.1016/j.jalz.2011.03.005.
31. Tijms BM, et al. Unbiased approach to counteract upward drift in cerebrospinal fluid Amyloid-β 1–42 analysis results. Clin Chem. 2018;64:576–85. https://doi.org/10.1373/clinchem.2017.281055.
32. Duits FH et al. The cerebrospinal fluid Alzheimer profile: Easily said, but what does it mean? Alzheimer's & Dementia 10, 713–e723712 (2014). https://doi.org/10.1016/j.jalz.2013.12.023
33. Alcolea D, et al. Agreement of amyloid PET and CSF biomarkers for Alzheimer's disease on lumipulse. Ann Clin Transl Neurol. 2019;6:1815–24. https://doi.org/10.1002/acn3.50873.
34. Goos JD, et al. Incidence of cerebral microbleeds: a longitudinal study in a memory clinic population. Neurology. 2010;74:1954–60. https://doi.org/10.1212/WNL.0b013e3181e396ea.
35. Joseph-Mathurin N, et al. Longitudinal accumulation of cerebral microhemorrhages in dominantly inherited Alzheimer disease. Neurology. 2021;96:e1632–45. https://doi.org/10.1212/wnl.0000000000011542.
36. Zimmer JA, et al. Amyloid-Related imaging abnormalities with Donanemab in early symptomatic Alzheimer disease: secondary analysis of the TRAILBLAZER-ALZ and ALZ 2 randomized clinical trials. JAMA Neurol. 2025;82:461–9. https://doi.org/10.1001/jamaneurol.2025.0065.
37. Cummings J, et al. Lecanemab: appropriate use recommendations. J Prev Alzheimers Dis. 2023;10:362–77. https://doi.org/10.14283/jpad.2023.30.
38. Cordonnier C, et al. Prevalence and severity of microbleeds in a memory clinic setting. Neurology. 2006;66:1356–60. https://doi.org/10.1212/01.wnl.0000210535.20297.ae.
39. Fazekas F, Chawluk JB, Alavi A, Hurtig HI, Zimmerman R. A. MR signal abnormalities at 1.5 T in Alzheimer's dementia and normal aging. AJR Am J Roentgenol. 1987;149:351–6. https://doi.org/10.2214/ajr.149.2.351.
40. Hok AHYS, Willemse EAJ, Teunissen CE, Del Campo M. Guidelines for CSF processing and biobanking: impact on the identification and development of optimal CSF protein biomarkers. Methods Mol Biol. 2019;2044:27–50. https://doi.org/10.1007/978-1-4939-9706-0_2.
41. Proteomics O. Development and validation of customized PEA biomarker panels with clinical utility. (2021).
42. van Buuren S, Groothuis-Oudshoorn K. Mice: multivariate imputation by chained equations in R. J Stat Softw. 2011;45:1–67. https://doi.org/10.18637/jss.v045.i03.
43. Wu T, et al. ClusterProfiler 4.0: A universal enrichment tool for interpreting omics data. Innov (Camb). 2021;2:100141. https://doi.org/10.1016/j.xinn.2021.100141.
44. Mukaka MM. Statistics corner: A guide to appropriate use of correlation coefficient in medical research. Malawi Med J. 2012;24:69–71.
45. Zott B, Konnerth A. Impairments of glutamatergic synaptic transmission in Alzheimer's disease. Semin Cell Dev Biol. 2023;139:24–34. https://doi.org/10.1016/j.semcdb.2022.03.013.
46. Murphy-Royal C, et al. Surface diffusion of astrocytic glutamate transporters shapes synaptic transmission. Nat Neurosci. 2015;18:219–26. https://doi.org/10.1038/nn.3901.
47. Squadrani L, et al. Astrocytes enhance plasticity response during reversal learning. Commun Biology. 2024;7:852. https://doi.org/10.1038/s42003-024-06540-8.
48. Uhlén M, et al. Proteomics. Tissue-based map of the human proteome. Science. 2015;347:1260419. https://doi.org/10.1126/science.1260419.
49. Uhlen M, et al. Towards a knowledge-based human protein atlas. Nat Biotechnol. 2010;28:1248–50. https://doi.org/10.1038/nbt1210-1248.
50. Taylor X, et al. Amyloid-β (Aβ) immunotherapy induced microhemorrhages are linked to vascular inflammation and cerebrovascular damage in a mouse model of Alzheimer's disease. Mol Neurodegeneration. 2024;19:77. https://doi.org/10.1186/s13024-024-00758-0.
51. Chung S, et al. Plexin-A4 mediates amyloid-β–induced Tau pathology in Alzheimer's disease animal model. Prog Neurobiol. 2021;203:102075. https://doi.org/10.1016/j.pneurobio.2021.102075.
52. Khan A, Sharma P, Dahiya S, Sharma B, Plexins. Navigating through the neural regulation and brain pathology. Neurosci Biobehavioral Reviews. 2025;169:105999. https://doi.org/10.1016/j.neubiorev.2024.105999.
53. Palm F, Onozato ML, Luo Z, Wilcox CS. Dimethylarginine dimethylaminohydrolase (DDAH): expression, regulation, and function in the cardiovascular and renal systems. Am J Physiol Heart Circ Physiol. 2007;293:H3227–3245. https://doi.org/10.1152/ajpheart.00998.2007.
54. Gao Q, et al. DDAH1 promotes neurogenesis and neural repair in cerebral ischemia. Acta Pharm Sinica B. 2024;14:2097–118. https://doi.org/10.1016/j.apsb.2024.02.001. https://doi.org/https://doi.org/.
55. Andrabi SM, et al. Nitric oxide: physiological functions, delivery, and biomedical applications. Adv Sci. 2023;10:2303259. https://doi.org/10.1002/advs.202303259.
56. Zhao Y, et al. DDAH-1, via regulation of ADMA levels, protects against ischemia-induced blood-brain barrier leakage. Lab Invest. 2021;101:808–23. https://doi.org/10.1038/s41374-021-00541-5.
57. Zhao Y, et al. DDAH-1 via HIF-1 target genes improves cerebral ischemic tolerance after hypoxic preconditioning and middle cerebral artery occlusion-reperfusion. Nitric Oxide. 2020;95:17–28. https://doi.org/10.1016/j.niox.2019.12.004.
58. Li N, Worthmann H, Deb M, Chen S, Weissenborn K. Nitric oxide (NO) and asymmetric dimethylarginine (ADMA): their pathophysiological role and involvement in intracerebral hemorrhage. Neurol Res. 2011;33:541–8. https://doi.org/10.1179/016164111x13007856084403.
59. Tijms BM, et al. Cerebrospinal fluid proteomics in patients with Alzheimer's disease reveals five molecular subtypes with distinct genetic risk profiles. Nat Aging. 2024;4:33–47. https://doi.org/10.1038/s43587-023-00550-7.
60. Abu-Rumeileh S, et al. CSF biomarkers of neuroinflammation in distinct forms and subtypes of neurodegenerative dementia. Alzheimers Res Ther. 2019;12:2. https://doi.org/10.1186/s13195-019-0562-4.
61. Sklepkiewicz P, et al. Inhibition of Macrophage-Specific CHIT1 as an approach to treat airway remodeling in severe asthma. Int J Mol Sci. 2023;24. https://doi.org/10.3390/ijms24054719.
62. Patel S, Goyal A. Chitin and chitinase: role in pathogenicity, allergenicity and health. Int J Biol Macromol. 2017;97:331–8. https://doi.org/10.1016/j.ijbiomac.2017.01.042. https://doi.org/https://doi.org/.
63. Pinteac R, Montalban X, Comabella M. Chitinases and chitinase-like proteins as biomarkers in neurologic disorders. Neurol Neuroimmunol Neuroinflamm. 2021;8. https://doi.org/10.1212/nxi.0000000000000921.
64. Yuan S, et al. CHIT1 regulates the neuroinflammation and phagocytosis of microglia and suppresses Aβ plaque deposition in Alzheimer's disease. J Pathol. 2025;265:330–41. https://doi.org/10.1002/path.6387.
65. van der Ende EL, et al. CSF proteomics in autosomal dominant Alzheimer's disease highlights parallels with sporadic disease. Brain. 2023;146:4495–507. https://doi.org/10.1093/brain/awad213.

66. Teunissen CE, et al. Methods to discover and validate Biofluid-Based biomarkers in neurodegenerative dementias. Mol Cell Proteom. 2023;22:100629. https://doi.org/10.1016/j.mcpro.2023.100629.
67. Pruitt KD, Tatusova T, Brown GR, Maglott DR. NCBI reference sequences (RefSeq): current status, new features and genome annotation policy. Nucleic Acids Res. 2012;40:D130–135. https://doi.org/10.1093/nar/gkr1079.
68. Dammer EB, et al. Multi-platform proteomic analysis of Alzheimer's disease cerebrospinal fluid and plasma reveals network biomarkers associated with proteostasis and the matrisome. Alzheimers Res Ther. 2022;14:174. https://doi.org/10.1186/s13195-022-01113-5.
69. Mavrina E, et al. Multi-Omics interdisciplinary research integration to accelerate dementia biomarker development (MIRIADE). Front Neurol. 2022;13. https://doi.org/10.3389/fneur.2022.890638.

Publisher's note